SAR Image De-noising Based on Non-local Similar Block Matching in NSST Domain

Hu Shaohai[1,2], Ma Xiaole[1,2], Liu Shuaiqi[3], Yang Dongsheng[1,2]
1. Institute of Information Science, Beijing Jiaotong University, Beijing 100044, China
2. Beijing Key Laboratory of Advanced Information Science and Network Technology, Beijing 100044, China
3. College of Electronic and Information Engineering, Hebei University, Baoding 071002, China
Email: shhu@bjtu.edu.cn, maxiaole@bjtu.edu.cn, shdkj-1918@163.com, dsyang@bjtu.edu.cn

***Abstract*—The traditional image de-noising in transform domain can get good de-noising effects, but it does not use the redundancy of the image information and the self-similarity of the image. In order to make full use of them and get better de-noising results, we propose a new SAR image de-noising method based on the non-local similar block matching in the non-subsampled shearlet domain. Firstly, we divide the image blocks into similar block groups with different characteristics by using the non-local similar block matching method; then, do the non-subsampled shearlet transform to every group and get the high and low frequency coefficients. Soft threshold is applied to the low frequency coefficients. Because the noise mainly exists in the high frequency component and the image coefficients in the transform domain have some correlation, we can define the adaptive threshold according to the correlation between the coefficients. Finally we can achieve the goal of the SAR image de-noising. The experimental results show that the proposed algorithm can keep more details about the original image and make less artificial texture. The proposed algorithm has stronger ability for image de-noising, and better visual effects.**

Keywords—SAR image de-noising; similar block matching; NSST; adaptive threshold de-noising

I. INTRODUCTION

Since the birth of the synthetic aperture radar (SAR) in the 1950s, because of the unique imaging characteristics such as high resolution, all-weather, all-time work, multi-polarization and so on, SAR image has the promising application in the military and civilian fields. However, due to the limitations of its coherent imaging mechanism, there is often some speckle in the final SAR image. In general, we need to use filtering processing technology to get the de-noised image [1].

At present, common de-noising methods of SAR image are image de-noising algorithms based on the transform domain. With the continuous development and improvement of the wavelet transform, it has become more and more widely applied in the image de-noising [2]. However, the two-dimensional wavelet only has the limited directions and cannot better express the two-dimensional images with line or surface [3,4]. To overcome the disadvantages above, various multi-scale geometric transforms have been put forward and the most popular one used in SAR image de-noising is contourlet [5]. But the contourlet does not have the shift invariance and its mathematical theory has some shortcomings. As the improvement of the contourlet [6], the non-subsampled contourlet transform has the shift invariance and can overcome the pseudo-gibbs artifacts, but it has large computation datas and it is time-consuming. So, according to the theory of the tight frame, Guo and Labate proposed the shearlet transform which is based on the strict mathematical logic reasoning [7]. Shearlet almost has the best non-linear error approximation order of the image, while its discretization needs down sampling operation. To overcome the shortcomings of the shearlet, the non-subsampled shearlet was proposed in [8]. NSST has the shift invariance and better directional selectivity. So it is better for the image de-noising.

Since every image has the self-similarity [9], it leads to the redundancy of the information in the image. NSST does not consider this similarity of the image, and its coefficients are not sparse. For better de-noising effects, we first divide the SAR image into many different image blocks of which the size are the same. Next, match the blocks into the image groups by using the non-local similar block matching. Then do the NSST transform to the different groups respectively and get the high frequency coefficients and low frequency coefficients. Finally deal the coefficients with different threshold values and do the inverse NSST transform to get the de-noised image.

The rest of this paper is organized as follows. Section 2 introduces the NSST. Section 3 describes the adaptive threshold in detail, including the signal-to-noise model and the adaptive threshold de-noising method. In Section 4, the complete procedure of the proposed algorithm is discussed and some experiments are designed to show the superiority of ours. At last, the conclusion is drawn in Section 5.

II. NON-SUBSAMPLED SHEARLET TRANSFORM

Combine the geometry with multi-resolution analysis by using the classical affine theory, and we can get the shearlet [7]. For the two-dimensional signal, the affine systems with composite dilations are:

$$A_{AB}(\psi)=\left\{\psi_{j,k,l}(x)=\left|\det A\right|^{\frac{j}{2}}\psi\left(B^{l}A^{j}x-k\right);\ j,l\in\mathbb{Z},k\in\mathbb{Z}^{2}\right\} \quad (1)$$

where $A=[4,0;0,2]$ denotes the anisotropic dilation matrix, $B=[1,1;0,1]$ denotes the shear matrix.

The support range of the function $\psi_{j,l,k}$ in the frequency domain is:

$$\sup p\,\widehat{\psi}^{(0)}_{j,l,k} \subset \left\{(\xi_1,\xi_2):\xi_1\in\left[-2^{2j-1},-2^{2j-4}\right]\cup \left[2^{2j-4},2^{2j-1}\right],\ \left|\xi_2/\xi_1+l2^{-j}\right|\le 2^{-j}\right\} \quad (2)$$

That is to say, the support range of $\widehat{\psi}^{(0)}_{j,l,k}$ is a pair of trapezoids, of which the approximate size is $2^{2j}\times 2^{j}$ and the slope is $l2^{-j}$. Suppose $D_0=\{(\xi_1,\xi_2)\in\hat{\mathbb{R}}^2:|\xi_1|\ge\frac{1}{8},|\frac{\xi_2}{\xi_1}|\le 1\}$, the function group [10] $\{\hat{\psi}^{(0)}(\xi A_0^{-j}B_0^{-l})\}$ forms a tiling of D_0 .

Therefore, the continuous shearlet transform can be defined as:

$$ST_{\psi}=\left\langle f,\psi^{(d)}_{j,l,k}\right\rangle \quad (3)$$

where $j\ge 0,-2^{j}\le l\le 2^{j}-1,k\in\mathbb{Z}^2,d=0,1$.

The discretization of NSST mainly includes the scale decomposition and direction decompositions. We can use the shear filter to realize the direction decomposition, while the scale decomposition can be implemented by non-subsampled pyramid (NSP) filter bank. After k levels NSP decomposition, we can get one low frequency sub-band and k high frequency sub-bands. Besides, all of these sub-bands have the same size as the original image. The NSST maps the standard shear filter from the pseudo polarization network system to the Cartesian coordinate system. As a result, it gives up the down sampling operation and it has the shift invariance. The detailed procedure is as follows:

Step 1: divide the image into the low frequency and high frequency images by using the NSP;

Step 2: structure the Meyer window for the high frequency image and do the multi-scale decomposition, and then we can get different directional sub-bands;

Step 3: deal each directional sub-band with inverse Fourier transform and get the final shear coefficients.

III. THE ADAPTIVE THRESHOLD DE-NOISING

A. The Signal-to-Noise Model

Normally, the speckle is fully developed [11]. So, the multiplicative model of it is as follows:

$$G(x,y)=F(x,y)\cdot N(x,y) \quad (4)$$

where $G(x,y)$ denotes the grey value polluted by the speckle at the position (x,y) ; $F(x,y)$ denotes the radar scattering characteristics of the ground targets. And $N(x,y)$ denotes the speckle noise caused by the decline, and it follows a Gamma distribution with the mean of one and variance of $1/L$.

When do the SAR image de-noising, we hope we can remove $N(x,y)$ and recover $F(x,y)$ from $G(x,y)$. For simplifying the process, we usually change the multiplicative model into an additive model by using the logarithmic transform seen as (5).

$$\ln[G(x,y)]=\ln[F(x,y)]+\ln[N(x,y)] \quad (5)$$

After the NSST transform, the signal-to-noise model in the transform domain can be expressed as follows:

$$G_{i,j}=F_{i,j}+N_{i,j} \quad (6)$$

where $G_{i,j}$ denotes the sub-band coefficients at the scale $\boldsymbol{i}$ and the direction $\boldsymbol{j}$. Accordingly, $F_{i,j}$ denotes the real image without the speckle, and $N_{i,j}$ denotes the speckle noise.

B. The Adaptive Threshold

Because the clear image $\ln[F(x,y)]$ and the noise $\ln[N(x,y)]$ are independent to each other, according to (6), we can get the equation below:

$$\sigma_G^2=\sigma_F^2+\sigma_N^2 \quad (7)$$

where σ_G^2 denotes the variance of the noisy image, σ_F^2 denotes the variance of the de-noised image and σ_N^2 denotes the noise variance. So, the noise variance in the sub-bands can be estimated by the following equation [12].

$$\hat{\sigma}_N=\frac{Median(\left|G_{i,j}\right|)}{0.6745} \quad (8)$$

Although we can achieve the goal of the image de-noising by the method above, the result is not the best because it does not consider the correlation between different pixels in the sub-bands. For better effects, we set the sliding window of which the center is $G_{i,j}(p,q)$ and the size is $N\times N$. Then we can get the variance of the pixel $G_{i,j}(p,q)$.

$$\hat{\sigma}^2_{G,p,q}=\frac{1}{N^2}\sum_{k=1}^{N}\sum_{l=1}^{N}\left|G_{i,j}(k,l)\right|^2 \quad (9)$$

The noise variance in the sub-bands of which the size is $m\times n$ can be estimated as follows:

$$\hat{\sigma}^2_G=\frac{1}{m\times n}\sum_{p=1}^{m}\sum_{q=1}^{n}\hat{\sigma}^2_{G,p,q} \quad (10)$$

Thus we can get the variance of the de-noised image. To guarantee the variance of the de-noised image is not negative, we get the variance of the pixel $F_{i,j}$ by (11).

$$\hat{\sigma}^2_F=\max((\hat{\sigma}^2_G-\hat{\sigma}^2_N),0) \quad (11)$$

So in the high frequency sub-bands, when we use the adaptive threshold to remove the noise, the threshold can be chosen as:

$$T_{i,j}(\hat{\sigma}_F^2) = \frac{\hat{\sigma}_N^2}{\hat{\sigma}_F} = \frac{\hat{\sigma}_N^2}{\sqrt{\max((\hat{\sigma}_G^2 - \hat{\sigma}_N^2), 0)}} \tag{12}$$

IV. SAR IMAGE DE-NOISING BASED ON NON-LOCAL SIMILAR BLOCK MATCHING IN NSST DOMAIN

A. Experimental Steps

In the proposed algorithm of this paper, we firstly match the noisy image blocks to get the similar block groups by using the non-local similar block matching method. Assuming the size of the reference block y_i is $\sqrt{m} \times \sqrt{m}$, we search the matching block y in the area of which the size is $D \times D$ and calculate the Euclidean distance between y and y_i. After that, rank the distances and we can get the first Q image blocks which will compose the similar block group Y_i. Among them, the Euclidean distance d can be calculated by the follow equation.

$$d(y, y_i) = \|y - y_i\|_2 \tag{13}$$

Then we do the logarithmic transform to the similar block groups, and after that we use the NSST transform to get the high frequency components and low frequency components. Finally we do the soft threshold to the low frequency components while doing the adaptive threshold to the high frequency components. At last, we can get the de-noised image by dealing the de-noised coefficients with inverse NSST transform and the exponential transform. More details can be seen in the Fig.1.

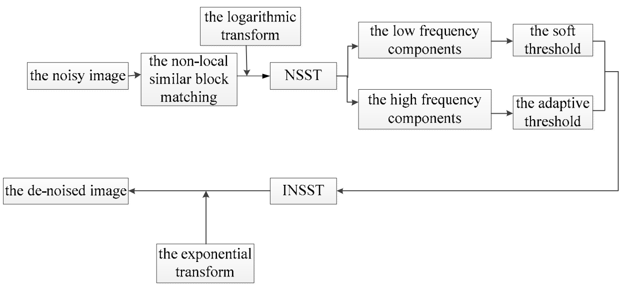

Fig.1. the flow chart of the proposed algorithm

B. Experimental Results

In order to verify the effectiveness and practicability of the proposed algorithm in this paper, we compare our algorithm with the classical SAR image de-noising based on shearlet transform (ST) in the transform domain [13], the image de-noising based on PPB [14] and the image de-noising based on SAR-BM3D [15]. In the experiments, when doing the non-local similar block matching, the size of each image block that we set is 16×16 which means $m = 256$, and the number of the image blocks in each similar block group is 20 which means $Q = 19$. When doing the adaptive threshold in the high frequency, the size of the sliding window we set is 8×8 which means $N = 8$. We do the experiments on the real SAR image taken by the Freanch Space Agency. Fig.2 (a) is the original image of which the size is 512×512, and (b) is the noisy image.

(a) The original image (b) The noisy image

Fig.2. the original and noisy image

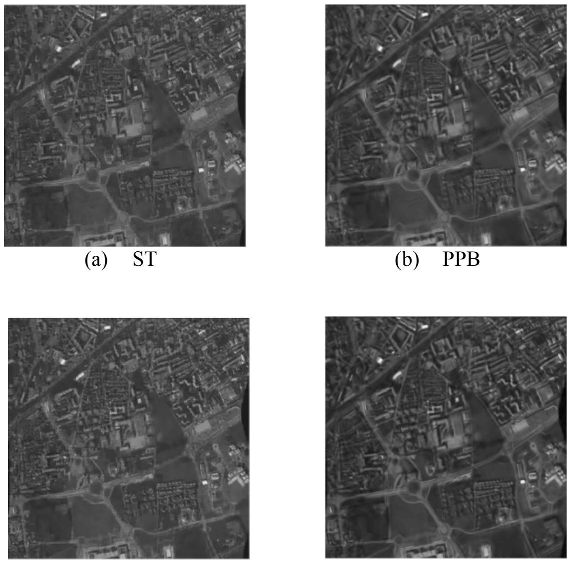

(a) ST (b) PPB

(c) SAR-BM3D (d) The proposed

Fig.3. the results of the different algorithms

Fig.3 shows the de-noised images by different algorithms. From the figure we can see, compared with the image de-noising based on ST, the PPB can remove the noise more effectively but it also makes some artificial texture. More details of the original image can be reserved by the SAR-BM3D, and the SAR-BM3D can suppress the artificial texture properly. However, compared with the proposed algorithm, the de-noised image by the SAR-BM3D is slightly fuzzy. Above all, the de-noised image by the proposed algorithm can not only reserve more details, suppress the artificial texture and edge blur, but also have better visual effects.

In order to evaluate the proposed algorithm more objectively, we will use some indexes [3], such as the peak signal-to-noise ratio (PSNR), equivalent number of looks (ENL), standard deviation (Sd) and structural similarity

(SSIM). Of all, the PSNR means the de-noising ability of the algorithm and the larger, the better. Greater the ENL is, better the visual effect of the de-noised image is; greater the SSIM is, more details of the original image can be reserved; while smaller the Sd is, the more robust the algorithm is. From Table 1 we can see, compared with other algorithms, the proposed algorithm in the paper has the highest PSNR, and the ENL and Sd are the best. What's more, the SSIM also is better

Table 1 the indexes of different algorithms

	PSNR	ENL	Sd	SSIM
ST	26.0538	5.0305	25.0805	0.8991
PPB	26.4646	5.3542	23.2979	0.9041
SAR-BM3D	26.5151	5.5681	26.3192	0.9118
The proposed	27.4609	5.5873	27.1027	0.9247

To show the superiority of the proposed algorithm more convincingly, we use another SAR image of which the size is also 512×512. Similar to the experiment above, Fig.4 (a) is the original image, while Fig.4 (b) is the noisy image.

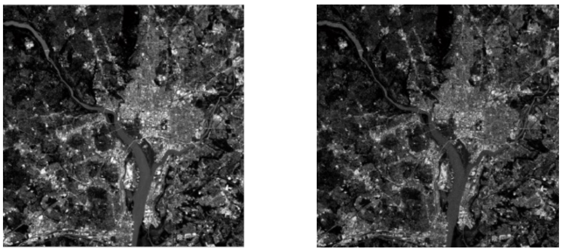

(a) The original image (b) The noisy image

Fig.4 the original and noisy image

The de-noised images by different algorithms above can be seen in the Fig.5. And Table 2 shows the values of the objective evaluation indexes by different algorithms. From the results we can see, the de-noised image of the proposed algorithm is best. It has less speckle noise and better visual effect. By using the proposed algorithm, more detail of the original image can be reserved and it produces less artificial texture. What's more, the proposed algorithm can greatly improve the PSNR of the de-noised image and the Sd is the smallest. At last, the ENL and SSIM of the proposed algorithm is largest

Table 2 the indexes of different algorithms

	PSNR	ENL	Sd	SSIM
ST	21.8264	4.0135	49.7477	0.9374
PPB	22.0319	4.9814	49.2390	0.9434
SAR-BM3D	22.0904	5.0424	49.5923	0.9428
The proposed	22.2745	5.2356	48.4959	0.9472

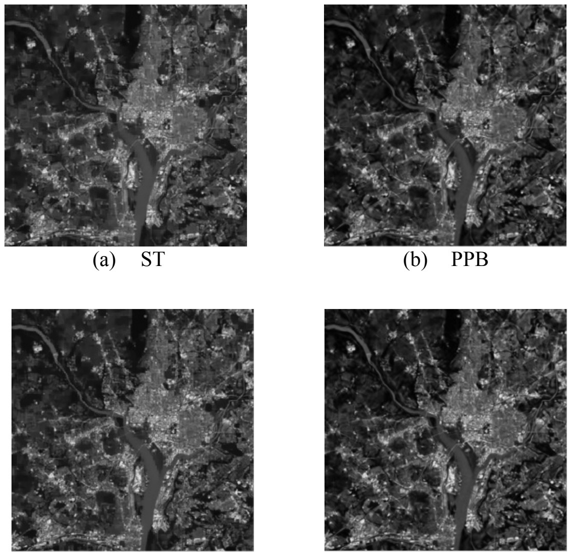

(a) ST (b) PPB

(c) SAR-BM3D (d) The proposed

Fig.5 the results of the different algorithms

V. CONCLUSION

In this paper, we propose a new SAR image de-noising algorithm based on non-local similar block matching in NSST domain. As we can see in the experiments, our algorithm is optimal. On the one hand, our algorithm improves the objective evaluation results and has better de-noising ability. On the other hand, the de-noised image by our algorithm has better visual effects. However the proposed algorithm is also imperfect, because of the time-consuming searching of all the image blocks and the calculating of Euclidean distance. Therefore, the future works will be the solving of the shortcomings remaining.

ACKNOWLEDGEMENTS

This work is supported by the Natural Science Foundation of China (No.61401308 and 61572063) and the Fundamental Research Funds for the Central Universities (No. 2016YJS039).

REFERENCES

[1] S.Q. Liu, P. Geng, M.Z. Shi, et al. SAR image de-noising based on generalized non-local means in non-subsample shearlet domain [C]. CSPS 15, Chengdu, Springer, 1-8.

[2] S.Q. Liu, S.H. Hu, Y. Xiao. SAR Image De-noised Based on Wavelet-Contourlet Transform with Cycle Spinning [J]. Signal Processing, 2011, 27(6): 837-842.

[3] S.Q. Liu, S.H. Hu, Y. Xiao. Bayesian shearlet shrinkage for SAR image de-noising via sparse representation [J]. Multidimensional Systems and Signal Processing, 2014, 25(4): 683-701.

[4] Martí-Cardona B, López-Martínez C, Dolz-Ripollés J. Local Isotropy Indicator for SAR Image Filtering: Application to Envisat/ASAR Images of the Doñana Wetland (November 2014) [J]. IEEE Journal of Selected Topics in Applied Earth Observations and Remote Sensing, 2015, 8(4): 1614-1622.

[5] S.Q. Liu, M.Z. Shi, S.H. Hu, et al. Synthetic aperture radar image de-noising based on Shearlet transform using the context-based model [J], Physical Communication, 2014,13(PartC):221-229.

[6] X.B. Qu, J.W. Yan, H.Z. Xiao, et al. Image Fusion Algorithm Based on

Spatial Frequency-Motivated Pulse Coupled Neural Networks in Nonsubsampled Contourlet Transform Domain [J]. Acta Automatica Sinica, 2008, 34(12): 1508-1514.
[7] K. Guo, D. Labate. Optimally sparse multidimensional representation using Shearlets [J]. SIAM Journal on Mathematical Analysis, 2007, 39(1): 298-318.
[8] G. Easley, D. Labate, W.Q. Lim. Sparse directional image representation using the discrete Shearlets transform [J]. Applied and Computational Harmonic Analysis, 2008, 25(1): 25-46.
[9] A. Buades, B. Coll, J.M. Morel. A review of image denoising algorithms, with a new one [J]. Multiscale Model. Simul., 2005, 4(2): 490-530.
[10] W.Q. Lim. The discrete Shearlets transform: a new directional transform and compactly supported Shearlets frames [J]. IEEE Transactions on Image Processing, 2010, 19(5):1166-1180.
[11] J.W. Goodman. Some fundamental properties of speckle [J]. Journal of the optical society of America, 1976, 66(11): 1145-1150.
[12] D.M. Li, L.J. Zhang, J.H. Yang, et al. Research on wavelet-based contourlet transform algorithm for adaptive optics image denoising [J]. Optik-International Journal for Light and Electron Optics, 2016, 127(12): 5029-5034.
[13] S.Q. Liu, S.H. Hu, Y. Xiao. SAR image de-noising based on Shearlet transform [J]. Journal of Applied Science, 2012, 30(6): 629-634.
[14] C. Deledalle, L. Denis, F. Tupin. Iterative weighted maximum likelihood denoising with probabilistic patch-based weights [J]. IEEE Trans. Image Process., 2009, 18(12): 2661-2672.
[15] S. Parrilli, M. Poderico, C. V. Angelino, et al. A nonlocal SAR image denoising algorithm based on LLMMSE wavelet shrinkage[J]. IEEE Trans. Geosci. Remote Sens., 2012, 50(2): 606-616.